Vacuum fluctuation effects on asymmetric nuclear matter

X.-H. Guo[1,*], B. Liu[2,†], and M.-H. Weng[1,‡]

[1] *College of Nuclear Science and Technology, Beijing Normal University, Beijing 100875, China*

[2] *Institute of High Energy Physics, Chinese Academy of Sciences, Beijing 100049, China*

The vacuum fluctuation (VF) effects on asymmetric nuclear matter are investigated. Masses of nucleons and mesons are modified in the nuclear medium by calculating the loop-diagram corrections and the density dependence of hadron masses is obtained. The relativistic Lagrangian density with the isovector scalar δ meson is used to calculate the nuclear equation of state (EOS) in the framework of the relativistic mean-field (RMF) approach, the effects of the in-medium hadron masses on the properties of neutron stars are finally studied. With the inclusion of the VF corrections, the nuclear EOS becomes softer and the neutron star masses are reduced.

PACS numbers: 21.30.Cb, 21.65.Cd, 21.60.Jz, 26.60.Kp

I. Introduction

The relativistic mean-field theory (RMF) [1, 2], which is one of the main applications of quantum hadrodynamics (QHD), is successful in nuclear structure studies [3, 4, 5]. The nonlinear (NL) Walecka model (NLWM), based on the RMF approach, has been extensively used to study the properties of nuclear and neutron matter, β-stable nuclei, and then extended to the drip-line regions [6, 7, 8, 9, 10, 11, 12]. In recent years some authors [11, 12, 13, 14, 15] have stressed the importance of including the scalar isovector virtual $\delta(a_0(980))$ field in hadronic effective field theories when asymmetric nuclear matter is studied. The inclusion of the δ meson leads to the structure of relativistic interactions, where a balance between an attractive (scalar) and a repulsive (vector) potential exists. The δ meson plays the role in the isospin channel and mainly affects the behavior of the system at high density regions and so is of great interest in nuclear astrophysics.

The properties of nuclear matter at high density play a crucial role for building models of neutron stars (NS). Neutron stars are objects of highly compressed matter. The structure of a compact star is characterized by its mass and radius, which are obtained from appropriate equation of state (EOS) at high densities. The EOS can be derived either from relativistic or potential models.

In order to describe the medium dependence of nuclear interactions, a density dependent relativistic hadron (DDRH) field theory has been recently proposed [16, 17, 18, 19]. Recently the authors [16] used the density dependent coupling models with the δ meson being included to study the neutron stars. They found that the introduction of the δ meson in the constant coupling model leads to heavier neutron stars in a nucleon-lepton picture. The neutron star masses in the density dependent models can be reduced when the δ meson is taken into account.

The in-medium modification to the masses of σ, ω, and ρ mesons has been studied in experiments

* *E-mail address:* xhguo@bnu.edu.cn
† *E-mail address:* liub@mail.ihep.ac.cn
‡ Corresponding author, *E-mail address:* mhweng@mail.bnu.edu.cn

and theoretical approaches for a decade [20, 21, 22, 23, 24, 25, 26]. Recently the authors of Ref. [27] investigated the effect of in-medium meson masses on the properties of the nuclear matter in the Walecka model and the effective masses of σ and ω mesons in the nuclear medium were calculated by taking into account the effects of the vacuum fluctuation (VF). In this work we want to see the VF effects on asymmetric matter and neutron stars. We also want to clarify the density dependence of in-medium nucleon and meson masses. The VF effects are naturally introduced by considering loop corrections to the self-energies of in-medium nucleons and mesons. The effective masses of nucleons and mesons (σ, ω, ρ, and δ) in the nuclear medium will be calculated in the VF-RMF model. The VF effects on asymmetric matter and neutron stars will be studied.

This paper is organized as follows. In Sec. II, we derive the in-medium effective masses of nucleons and mesons and the EOS for nuclear matter in VF-RMF model. In Sec. III, we compare our results with those of the NL-RMF model. In Sec. IV, a brief summary is presented.

II. Hadron effective masses and EOS of nuclear matter

The relativistic Lagrangian density of the interacting many-particle system consisting of nucleons, isoscalar (scalar σ, vector ω), and isovector (scalar δ, vector ρ) mesons used in this work is

$$\begin{aligned}\mathcal{L} \;=\; & \bar{\psi}\Big[i\gamma^\mu\partial_\mu - g_\omega\gamma^\mu\omega_\mu - g_\rho\gamma^\mu\vec{\tau}\cdot\vec{b}_\mu - (M - g_\sigma\phi - g_\delta\vec{\tau}\cdot\vec{\delta})\Big]\psi \\ & + \frac{1}{2}(\partial_\mu\phi\partial^\mu\phi - m_\sigma^2\phi^2) - U(\phi) + \frac{1}{2}m_\omega^2\omega_\mu\omega^\mu \\ & + \frac{1}{2}m_\rho^2\vec{b}_\mu\cdot\vec{b}^\mu + \frac{1}{2}(\partial_\mu\vec{\delta}\partial^\mu\vec{\delta} - m_\delta^2\vec{\delta}^2) \\ & - \frac{1}{4}F_{\mu\nu}F^{\mu\nu} - \frac{1}{4}\vec{G}_{\mu\nu}\vec{G}^{\mu\nu} + \delta\mathcal{L}, \end{aligned} \tag{1}$$

where ϕ, ω_μ, $\vec{b}_\mu$, and $\vec{\delta}$ represent σ, ω, ρ, and δ meson fields, respectively, $U(\phi) = \frac{1}{3}a\phi^3 + \frac{1}{4}b\phi^4$ is the nonlinear potential of the σ meson, $F_{\mu\nu} \equiv \partial_\mu\omega_\nu - \partial_\nu\omega_\mu$, and $\vec{G}_{\mu\nu} \equiv \partial_\mu\vec{b}_\nu - \partial_\nu\vec{b}_\mu$. In order to remove the divergence in the loop calculation, the counterterm for the Lagrangian density, $\delta\mathcal{L}$, included in Eq. (1) reads

$$\begin{aligned}\delta\mathcal{L} \;=\; & \alpha_1\phi + \frac{1}{2!}\alpha_2\phi^2 + \frac{1}{3!}\alpha_3\phi^3 + \frac{1}{4!}\alpha_4\phi^4 + \frac{\zeta_\sigma}{2}(\partial\phi)^2 \\ & + \beta_1\vec{\delta} + \frac{1}{2!}\beta_2\vec{\delta}^2 + \frac{1}{3!}\beta_3\vec{\delta}^3 + \frac{1}{4!}\beta_4\vec{\delta}^4 + \frac{\zeta_\delta}{2}(\partial\vec{\delta})^2 \\ & + \frac{\zeta_\omega}{2}(\partial\omega_\mu)^2 + \frac{\zeta_\rho}{2}(\partial\vec{b}_\mu)^2, \end{aligned} \tag{2}$$

where the parameters α_i, β_i, and ζ_j (i=1, 2, 3, 4; j=σ, ω, ρ, δ) are fixed by the renormalization methods suggested in Refs. [2, 28].

The field equations in the RMF approximation are

$$
\begin{aligned}
[i\gamma^{\mu}\partial_{\mu}-(M-g_{\sigma}\phi-g_{\delta}\tau_{3}\delta_{3})-g_{\omega}\gamma^{0}\omega_{0}-g_{\rho}\gamma^{0}\tau_{3}b_{0}]\psi &= 0,\\
m_{\sigma}^{2}\phi+a\phi^{2}+b\phi^{3} &= g_{\sigma}\rho^{s},\\
m_{\omega}^{2}\omega_{0} &= g_{\omega}\rho,\\
m_{\rho}^{2}b_{0} &= g_{\rho}\rho_{3},\\
m_{\delta}^{2}\delta_{3} &= g_{\delta}\rho_{3}^{s},
\end{aligned}
\tag{3}
$$

where $\rho^{(s)}=\rho_{p}^{(s)}+\rho_{n}^{(s)}$ and $\rho_{3}^{(s)}=\rho_{p}^{(s)}-\rho_{n}^{(s)}$, where ρ_i and ρ_i^s (the index (subscript or superscript) i denotes proton or neutron throughout this paper) are the nucleon and scalar densities, respectively.

The nucleon and the scalar densities are given by, respectively,

$$
\rho_{i} = \frac{k_{F_i}^{3}}{3\pi^{2}},
\tag{4}
$$

and

$$
\rho_{i}^{s} = -i\int\frac{\mathrm{d}^{4}k}{(2\pi)^{4}}\mathrm{Tr}G^{i}(k),
\tag{5}
$$

where k_{F_i} is the Fermi momentum of the nucleon and $G^i(k)$ is the nucleon propagator in the VF-RMF model:

$$
\begin{aligned}
G^{i}(k) &= (\gamma_{\mu}k^{\mu}+M_{i}^{\star})\Big[\frac{1}{k^{2}-M_{i}^{\star 2}+i\eta}+\frac{i\pi}{E_{F_i}^{\star}}\delta(k^{0}-E_{F_i})\theta(k_{F_i}-|\vec{k}|)\Big]\\
&\equiv G_{F}^{i}(k)+G_{D}^{i}(k),
\end{aligned}
\tag{6}
$$

where $E_{F_i}^{\star}=\sqrt{k_{F_i}^{2}+M_{i}^{\star 2}}$, $M_i^{\star}$ is the nucleon effective masses, and η is infinitesimal. Here $G_F^i(k)$ describes the free propagation of positive and negative energy quasi-nucleons. $G_D^i(k)$ describes quasi-nucleon 'holes' inside the Fermi sea and corrects the propagation of positive energy quasi-nucleons by the Pauli exclusion principle.

The nucleon effective mass without the δ field in the RMF approach is $M^{\star}=M-g_{\sigma}\phi$. When the VF effects are considered, the loop-diagram corrections to the self-energy of nucleons and mesons shown in Fig. 1 are naturally introduced. The nucleon effective mass without the δ field in the RMF approach including the vacuum fluctuations can be calculated from Fig. 1(a). Thus, we have

$$
\begin{aligned}
M^{\star} &= M+\frac{ig_{\sigma}^{2}}{m_{\sigma}^{\star 2}}\int\frac{\mathrm{d}^{4}k}{(2\pi)^{4}}[\mathrm{Tr}G^{p}(k)+\mathrm{Tr}G^{n}(k)]+\frac{a}{m_{\sigma}^{\star 2}g_{\sigma}}(M^{\star}-M)^{2}-\frac{b}{m_{\sigma}^{\star 2}g_{\sigma}^{2}}(M^{\star}-M)^{3}\\
&= M-\frac{g_{\sigma}^{2}}{2\pi^{2}m_{\sigma}^{\star 2}}\Big[k_{F_p}M^{\star}E_{F_p}^{\star}-M^{\star 3}\ln(\frac{k_{F_p}+E_{F_p}^{\star}}{M^{\star}})\Big]\\
&\quad-\frac{g_{\sigma}^{2}}{2\pi^{2}m_{\sigma}^{\star 2}}\Big[k_{F_n}M^{\star}E_{F_n}^{\star}-M^{\star 3}\ln(\frac{k_{F_n}+E_{F_n}^{\star}}{M^{\star}})\Big]\\
&\quad+\frac{g_{\sigma}^{2}}{\pi^{2}m_{\sigma}^{\star 2}}\Big[M^{\star 3}\ln(\frac{M^{\star}}{M})-M^{2}(M^{\star}-M)-\frac{5}{2}M(M^{\star}-M)^{2}-\frac{11}{6}(M^{\star}-M)^{3}\Big]\\
&\quad+\frac{a}{m_{\sigma}^{\star 2}g_{\sigma}}(M^{\star}-M)^{2}-\frac{b}{m_{\sigma}^{\star 2}g_{\sigma}^{2}}(M^{\star}-M)^{3},
\end{aligned}
\tag{7}
$$

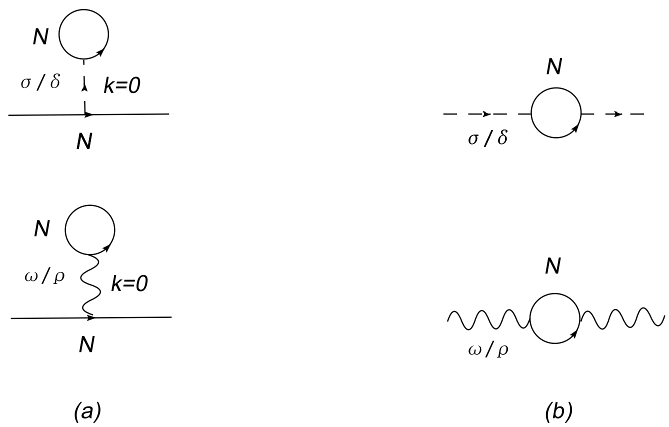

FIG. 1: Loop-diagram corrections to the self-energy of nucleons (a) and mesons (b) in nuclear medium, where N denotes nucleon and k is the four momentum of the meson.

where the second term in the right hand side of the first line in Eq. (7) is given by Fig. 1(a), and the third and fourth terms are the contributions from the nonlinear potential of the σ meson.

As well known, the δ meson leads to a definite splitting of proton and neutron effective masses, the nucleon effective masses with the δ meson in the RMF approach are given by, respectively,

$$M_p^\star = M - g_\sigma\phi - g_\delta\delta_3, \tag{8}$$

and

$$M_n^\star = M - g_\sigma\phi + g_\delta\delta_3. \tag{9}$$

The nucleon effective masses with the δ meson in the RMF approach including the vacuum fluctuations can be calculated from Fig. 1(a),

$$\begin{aligned} M_p^\star &= M - g_\sigma\phi - g_\delta\delta_3 \\ &= M + \frac{ig_\sigma^2}{m_\sigma^{\star 2}}\int\frac{\mathrm{d}^4k}{(2\pi)^4}[\mathrm{Tr}G^p(k) + \mathrm{Tr}G^n(k)] \\ &+ \frac{ig_\delta^2}{m_\delta^{\star 2}}\int\frac{\mathrm{d}^4k}{(2\pi)^4}[\mathrm{Tr}G^p(k) - \mathrm{Tr}G^n(k)] \\ &- a\frac{2g_\sigma^2}{m_\sigma^{\star 2}}\frac{(M_p^\star + M_n^\star - 2M)^2}{(-2g_\sigma)^3} - b\frac{2g_\sigma^2}{m_\sigma^{\star 2}}\frac{(M_p^\star + M_n^\star - 2M)^3}{(-2g_\sigma)^4}, \end{aligned} \tag{10}$$

and

$$\begin{aligned} M_n^\star &= M - g_\sigma\phi + g_\delta\delta_3 \\ &= M + \frac{ig_\sigma^2}{m_\sigma^{\star 2}}\int\frac{\mathrm{d}^4k}{(2\pi)^4}[\mathrm{Tr}G^n(k) + \mathrm{Tr}G^p(k)] \\ &+ \frac{ig_\delta^2}{m_\delta^{\star 2}}\int\frac{\mathrm{d}^4k}{(2\pi)^4}[\mathrm{Tr}G^n(k) - \mathrm{Tr}G^p(k)] \\ &- a\frac{2g_\sigma^2}{m_\sigma^{\star 2}}\frac{(M_p^\star + M_n^\star - 2M)^2}{(-2g_\sigma)^3} - b\frac{2g_\sigma^2}{m_\sigma^{\star 2}}\frac{(M_p^\star + M_n^\star - 2M)^3}{(-2g_\sigma)^4}. \end{aligned} \tag{11}$$

Thus, we get after the momentum integral

$$
\begin{aligned}
M_p^\star &= M - \frac{1}{2\pi^2}(\frac{g_\sigma^2}{m_\sigma^{\star 2}} + \frac{g_\delta^2}{m_\delta^{\star 2}})\Big[k_{F_p} M_p^\star E_{F_p}^\star - M_p^{\star 3}\ln(\frac{k_{F_p} + E_{F_p}^\star}{M_p^\star})\Big] \\
&+\frac{1}{2\pi^2}(\frac{g_\sigma^2}{m_\sigma^{\star 2}} + \frac{g_\delta^2}{m_\delta^{\star 2}})\Big[M_p^{\star 3}\ln(\frac{M_p^\star}{M}) - M^2(M_p^\star - M) \\
&-\frac{5}{2}M(M_p^\star - M)^2 - \frac{11}{6}(M_p^\star - M)^3\Big] \\
&-\frac{1}{2\pi^2}(\frac{g_\sigma^2}{m_\sigma^{\star 2}} - \frac{g_\delta^2}{m_\delta^{\star 2}})\Big[k_{F_n} M_n^\star E_{F_n}^\star - M_n^{\star 3}\ln(\frac{k_{F_n} + E_{F_n}^\star}{M_n^\star})\Big] \\
&+\frac{1}{2\pi^2}(\frac{g_\sigma^2}{m_\sigma^{\star 2}} - \frac{g_\delta^2}{m_\delta^{\star 2}})\Big[M_n^{\star 3}\ln(\frac{M_n^\star}{M}) - M^2(M_n^\star - M) \\
&-\frac{5}{2}M(M_n^\star - M)^2 - \frac{11}{6}(M_n^\star - M)^3\Big] \\
&-a\frac{2g_\sigma^2}{m_\sigma^{\star 2}}\frac{(M_p^\star + M_n^\star - 2M)^2}{(-2g_\sigma)^3} - b\frac{2g_\sigma^2}{m_\sigma^{\star 2}}\frac{(M_p^\star + M_n^\star - 2M)^3}{(-2g_\sigma)^4},
\end{aligned} \tag{12}
$$

and

$$
\begin{aligned}
M_n^\star &= M - \frac{1}{2\pi^2}(\frac{g_\sigma^2}{m_\sigma^{\star 2}} - \frac{g_\delta^2}{m_\delta^{\star 2}})\Big[k_{F_p} M_p^\star E_{F_p}^\star - M_p^{\star 3}\ln(\frac{k_{F_p} + E_{F_p}^\star}{M_p^\star})\Big] \\
&+\frac{1}{2\pi^2}(\frac{g_\sigma^2}{m_\sigma^{\star 2}} - \frac{g_\delta^2}{m_\delta^{\star 2}})\Big[M_p^{\star 3}\ln(\frac{M_p^\star}{M}) - M^2(M_p^\star - M) \\
&-\frac{5}{2}M(M_p^\star - M)^2 - \frac{11}{6}(M_p^\star - M)^3\Big] \\
&-\frac{1}{2\pi^2}(\frac{g_\sigma^2}{m_\sigma^{\star 2}} + \frac{g_\delta^2}{m_\delta^{\star 2}})\Big[k_{F_n} M_n^\star E_{F_n}^\star - M_n^{\star 3}\ln(\frac{k_{F_n} + E_{F_n}^\star}{M_n^\star})\Big] \\
&+\frac{1}{2\pi^2}(\frac{g_\sigma^2}{m_\sigma^{\star 2}} + \frac{g_\delta^2}{m_\delta^{\star 2}})\Big[M_n^{\star 3}\ln(\frac{M_n^\star}{M}) - M^2(M_n^\star - M) \\
&-\frac{5}{2}M(M_n^\star - M)^2 - \frac{11}{6}(M_n^\star - M)^3\Big] \\
&-a\frac{2g_\sigma^2}{m_\sigma^{\star 2}}\frac{(M_p^\star + M_n^\star - 2M)^2}{(-2g_\sigma)^3} - b\frac{2g_\sigma^2}{m_\sigma^{\star 2}}\frac{(M_p^\star + M_n^\star - 2M)^3}{(-2g_\sigma)^4},
\end{aligned} \tag{13}
$$

where $m_j^\star$ $(j = \sigma, \omega, \rho, \delta)$ are the in-medium meson masses.

The effective mass of the meson (or in-medium meson mass) is defined as the pole position of the meson propagator at zero three-momentum (on-shell) or zero four-momentum (off-shell). We calculate the in-medium meson masses in the random phase approximation (RPA) [27, 28]. The corresponding diagrams are given in Fig. 1(b). Thus, we obtain the in-medium masses of scalar mesons:

$$
m_j^{\star 2} = m_j^2 + \Pi_j(q^\mu) \;\; (j = \sigma, \delta), \tag{14}
$$

where

$$
\Pi_j(q^\mu) = -ig_j^2 \sum_{i=n,p} \int \frac{\mathrm{d}^4 k}{(2\pi)^4} \mathrm{Tr} G^i(k+q) G^i(k). \tag{15}
$$

The expressions of Π_j (on-shell and off-shell) are, respectively,

$$\Pi_j(\vec{q}=0;q^0=m_j^\star) \;=\; \frac{g_j^2}{4\pi^2}\sum_{i=n,p}\Big[\frac{1}{m_j^\star}(4M_i^{\star 2}-m_j^{\star 2})^{3/2}\arctan(\frac{m_j^\star k_{F_i}}{E_{F_i}^\star\sqrt{4M_i^{\star 2}-m_j^{\star 2}}})$$

$$+(m_j^{\star 2}-6M_i^{\star 2})\ln\Big(\frac{k_{F_i}+E_{F_i}^\star}{M_i^\star}\Big)+2k_{F_i}E_{F_i}^\star\Big]$$

$$-\frac{g_j^2}{2\pi^2}\sum_{i=n,p}\Big\{\frac{3}{2}(M_i^{\star 2}-M^2)\int_0^1 \mathrm{d}x\ln\Big(1-\frac{m_j^2}{M^2}x(1-x)\Big)$$

$$+\frac{3}{2}\int_0^1 \mathrm{d}x\Big[(M_i^{\star 2}-m_j^{\star 2}x(1-x))\ln\Big(\frac{M_i^{\star 2}-m_j^{\star 2}x(1-x)}{M^2-m_j^2x(1-x)}\Big)\Big]$$

$$-\frac{m_j^2-m_j^{\star 2}}{4}-3M(M_i^\star-M)-\frac{9}{2}(M_i^\star-M)^2\Big\}, \tag{16}$$

and

$$\Pi_j(q^\mu=0) \;=\; \frac{g_j^2}{2\pi^2}\sum_{i=n,p}\Big[\frac{3M_i^{\star 2}k_{F_i}+k_{F_i}^3}{E_{F_i}^\star}-3M_i^{\star 2}\ln\Big(\frac{k_{F_i}+E_{F_i}^\star}{M_i^\star}\Big)\Big]$$

$$-\frac{3g_j^2}{4\pi^2}\sum_{i=n,p}\Big[2M_i^{\star 2}\ln\Big(\frac{M_i^\star}{M}\Big)-M^2+4MM_i^\star-3M_i^{\star 2}\Big]. \tag{17}$$

The effective masses of vector mesons can be obtained from Fig. 1(b)

$$m_j^{\star 2}=m_j^2+\Pi_{jT}(q^\mu) \quad (j=\omega,\rho), \tag{18}$$

where Π_{jT} is the transverse part of the polarization tensor as follows:

$$\Pi_{\mu\nu}(q^\mu)=-ig_j^2\sum_{i=n,p}\int\frac{\mathrm{d}^4k}{(2\pi)^4}\mathrm{Tr}\gamma_\mu G^i(k+q)\gamma_\nu G^i(k). \tag{19}$$

So the expressions of Π_{jT} (on-shell and off-shell) are, respectively,

$$\Pi_{jT}(\vec{q}=0;q^0=m_j^\star) \;=\; -\frac{g_j^2}{6\pi^2}\sum_{i=n,p}\Big[\frac{8M_i^{\star 4}+2M_i^{\star 2}m_j^{\star 2}-m_j^{\star 4}}{m_j^\star\sqrt{4M_i^{\star 2}-m_j^{\star 2}}}\arctan\Big(\frac{m_j^\star k_{F_i}}{E_{F_i}^\star\sqrt{4M_i^{\star 2}-m_j^{\star 2}}}\Big)$$

$$-2k_{F_i}E_{F_i}^\star-m_j^{\star 2}\ln\Big(\frac{k_{F_i}+E_{F_i}^\star}{M_i^\star}\Big)\Big]$$

$$-\frac{g_j^2m_j^{\star 2}}{2\pi^2}\sum_{i=n,p}\int_0^1 \mathrm{d}x x(x-1)\ln\Big[\frac{M_i^{\star 2}-m_j^{\star 2}x(1-x)}{M^2-m_j^2x(1-x)}\Big], \tag{20}$$

and

$$\Pi_{jT}(q^\mu=0)=\frac{g_j^2}{3\pi^2}\sum_{i=n,p}\frac{k_{F_i}^3}{E_{F_i}^\star}. \tag{21}$$

We note that the VF contributions are included in the second summations of $\Pi_j(q^\mu)$ and $\Pi_{jT}(q^\mu)$ (Eqs. (16), (17) and (20)), the VF contribution in Eq. (21) equals zero.

The in-medium meson propagator is significantly modified by the interaction of the mesons with the nucleons. Clearly, this modification of the meson propagators will change the nucleon effective mass as well as the energy density. The meson propagators in the tadpole diagram are calculated at zero four momentum transfer. So we must replace the meson mass appearing in the nucleon effective mass and the energy density by the meson effective mass defined as [27]:

$$m_j^{\star 2} = m_j^2 + \Pi_j(q^\mu = 0) \ \ (j = \sigma, \delta), \tag{22}$$

and

$$m_j^{\star 2} = m_j^2 + \Pi_{jT}(q^\mu = 0) \ \ (j = \omega, \rho). \tag{23}$$

Therefore, the energy-momentum tensor in the VF-RMF model can be expressed as

$$T_{\mu\nu} \ = \ i\bar{\psi}\gamma_\mu\partial_\nu\psi + g_{\mu\nu}\left[\frac{1}{2}m_\sigma^\star\phi^2 + \frac{1}{2}m_\delta^\star\vec{\delta}^2 - \frac{1}{2}m_\omega^\star\omega_\lambda\omega^\lambda - \frac{1}{2}m_\rho^\star\vec{b}_\lambda\vec{b}^\lambda + U(\phi)\right]. \tag{24}$$

Thus the EOS for nuclear matter in the VF-RMF model can be obtained. The energy density is given by

$$\begin{aligned} \varepsilon \ = \ & \langle T^{00}\rangle = \frac{g_\omega^2}{2m_\omega^{\star 2}}\rho^2 + \frac{g_\rho^2}{2m_\rho^{\star 2}}\rho_3^2 + \frac{1}{2}m_\sigma^{\star 2}\phi^2 + \frac{1}{2}m_\delta^{\star 2}\delta_3^2 \\ & + \frac{1}{8\pi^2}\sum_{i=n,p}\left[k_{F_i}E_{F_i}^\star(M_i^{\star 2} + 2k_{F_i}^2) - M_i^{\star 4}\ln(\frac{k_{F_i} + E_{F_i}^\star}{M_i^\star})\right] + U(\phi) \\ & - \frac{1}{8\pi^2}\sum_{i=n,p}\left[M_i^{\star 4}\ln(\frac{M_i^\star}{M}) + M^3(M - M_i^\star) - \frac{7}{2}M^2(M - M_i^\star)^2 \right. \\ & \left. + \frac{13}{3}M(M - M_i^\star)^3 - \frac{25}{12}(M - M_i^\star)^4\right], \end{aligned} \tag{25}$$

and the pressure is

$$\begin{aligned} P \ = \ & \frac{1}{3}\langle T^{ii}\rangle = \frac{g_\omega^2}{2m_\omega^{\star 2}}\rho^2 + \frac{g_\rho^2}{2m_\rho^{\star 2}}\rho_3^2 - \frac{1}{2}m_\sigma^{\star 2}\phi^2 - \frac{1}{2}m_\delta^{\star 2}\delta_3^2 \\ & + \frac{1}{8\pi^2}\sum_{i=n,p}\left[M_i^{\star 4}\ln(\frac{k_{F_i} + E_{F_i}^\star}{M_i^\star}) - E_{F_i}^\star k_{F_i}(M_i^{\star 2} - \frac{2}{3}k_{F_i}^2)\right] - U(\phi) \\ & + \frac{1}{8\pi^2}\sum_{i=n,p}\left[M_i^{\star 4}\ln(\frac{M_i^\star}{M}) + M^3(M - M_i^\star) - \frac{7}{2}M^2(M - M_i^\star)^2 \right. \\ & \left. + \frac{13}{3}M(M - M_i^\star)^3 - \frac{25}{12}(M - M_i^\star)^4\right]. \end{aligned} \tag{26}$$

The density dependence of the nuclear symmetry energy, E_{sym}, is one of the basic properties of asymmetric nuclear matter for studying the structure of neutron stars. Empirically, we have information on E_{sym} only at the saturation point, where it ranges from 28 to 35 MeV according to

the nuclear mass table [29]. The nuclear symmetry energy is defined through the expansion of the binding energy in terms of the asymmetry parameter α [12]:

$$E/A(\rho,\alpha) = E/A(\rho,0) + E_{sym}(\rho)\alpha^2 + O(\alpha^4) + \cdots, \tag{27}$$

where the binding energy density is defined as $E/A = \varepsilon/\rho - M$, and the asymmetry parameter $\alpha = (\rho_n - \rho_p)/\rho$.

The nuclear symmetry energy is defined by

$$E_{sym} \equiv \frac{1}{2}\frac{\partial^2(E/A)}{\partial\alpha^2}\Big|_{\alpha=0} = \frac{1}{2}\rho\frac{\partial^2\varepsilon}{\partial\rho_3^2}\Big|_{\rho_3=0}. \tag{28}$$

According to the definition, an explicit expression for the symmetry energy in the VF-RMF model is obtained as

$$\begin{aligned} E_{sym} \; = \; & \frac{1}{2}\frac{g_\rho^2}{m_\rho^{\star 2}}\rho + \frac{1}{6}\frac{k_F^2}{E_F^\star} - \frac{1}{2}\frac{g_\delta^2}{m_\delta^{\star 2}}\frac{M^{\star 2}\rho}{E_F^{\star 2}(1+\frac{g_\delta^2}{m_\delta^{\star 2}}C - \frac{1}{\pi^2}\frac{g_\delta^2}{m_\delta^{\star 2}}D)} \\ & + \frac{\rho}{2\pi^2}\frac{g_\delta^4}{m_\delta^{\star 4}}\frac{M^{\star 2}}{E_F^{\star 2}}\frac{D}{1+\frac{g_\delta^2}{m_\delta^{\star 2}}C - \frac{1}{\pi^2}\frac{g_\delta^2}{m_\delta^{\star 2}}D} \\ & - \frac{\rho}{4\pi^2}\frac{g_\delta^4}{m_\delta^{\star 4}}\frac{M^{\star 2}}{E_F^{\star 2}}\frac{1}{(1+\frac{g_\delta^2}{m_\delta^{\star 2}}C - \frac{1}{\pi^2}\frac{g_\delta^2}{m_\delta^{\star 2}}D)^2}\Big[12M^{\star 2}\ln\frac{M^\star}{M} + 7M^{\star 2} \\ & -7M^2 + 26M(M-M^\star) - 25(M-M^\star)^2\Big], \end{aligned} \tag{29}$$

where

$$C = \frac{1}{\pi^2}\Big[\frac{k_F E_F^{\star 2} + 2M^{\star 2}k_F}{E_F^\star} - 3M^{\star 2}\ln\Big(\frac{k_F + E_F^\star}{M^\star}\Big)\Big], \tag{30}$$

and

$$D = 3M^{\star 2}\ln\frac{M^\star}{M} + M^{\star 2} - M^2 - 5M(M^\star - M) - \frac{11}{2}(M^\star - M)^2. \tag{31}$$

As discussed in Refs. [30, 31], the incompressibility K is one of the important ingredients for the nuclear EOS. The incompressibility of nuclear matter is defined by [30, 31]

$$K = 9\rho_0^2\frac{\partial^2(\varepsilon/\rho)}{\partial\rho^2}\Big|_{\rho=\rho_0} = 9\frac{\partial P}{\partial\rho}\Big|_{\rho=\rho_0} = 9\rho_0\frac{\partial\mu}{\partial\rho}\Big|_{\rho=\rho_0}, \tag{32}$$

where $\mu = (\varepsilon + P)/\rho$ is the baryon chemical potential and ρ_0 is the saturation density.

We can easily obtain the incompressibility from the EOS in the VF-RMF model as

$$K = 9\rho_0\Big(\frac{k_F^2}{3\rho E_F^\star} + \frac{g_\omega^2}{m_\omega^{\star 2}} + \frac{M^\star}{E_F^\star}\frac{\partial M^\star}{\partial\rho}\Big)\Big|_{\rho=\rho_0}, \tag{33}$$

where

$$\frac{\partial M^\star}{\partial \rho} = -\frac{g_\sigma^2}{m_\sigma^{\star 2}}\frac{M^\star}{E_F^\star}Q^{-1}, \tag{34}$$

and

$$\begin{aligned} Q &= 1+\frac{g_\sigma^2}{\pi^2 m_\sigma^{\star 2}}\Big(k_F E_F^\star + \frac{2k_F M^{\star 2}}{E_F^\star} - 3M^{\star 2}\ln(\frac{k_F+E_F^\star}{M}) + \frac{9}{2}M^{\star 2} + \frac{3}{2}M^2 - 6MM^\star\Big) \\ &+\frac{2a}{m_\sigma^{\star 2} g_\sigma}(M-M^\star) + \frac{3b}{m_\sigma^{\star 2} g_\sigma^2}(M-M^\star)^2. \end{aligned} \tag{35}$$

The final outcome of a supernova explosion can be a neutron star or a black hole. The neutron star is believed to evolve from an initially hot protoneutron star. The matter in cold neutron stars is in the ground state in nuclear equilibrium. Matter in equilibrium concerning weak interactions is called as β-equilibrium matter. The composition of β-equilibrium system is determined by the request of charge neutrality and chemical-potential equilibrium [30, 32]. The balance processes for β-equilibrium (npe) system are the following weak reactions:

$$n \longrightarrow p + e^- + \bar{\nu}_e, \tag{36}$$

$$p + e^- \longrightarrow n + \nu_e. \tag{37}$$

The chemical-potential equilibrium condition for (npe) system can be written as

$$\mu_e = \mu_n - \mu_p, \tag{38}$$

where the electron chemical-potential $\mu_e = \sqrt{k_{F_e}^2 + m_e^2}$, k_{F_e} is the electron momentum at the fermion level and m_e is the electron mass.

The charge neutrality condition is

$$\rho_e = \rho_p = X_p \rho, \tag{39}$$

where ρ_e is the electron density, and the proton fraction $X_p = Z/A = \rho_p/\rho$.

In the ultra-relativistic limit for noninteracting electrons, the electron density can be expressed as a function of its chemical potential

$$\rho_e = \frac{1}{3\pi^2}\mu_e^3. \tag{40}$$

Then, we can obtain the relation between the proton fraction X_p and the nuclear symmetry energy E_{sym}

$$3\pi^2 \rho X_p - [4E_{sym}(1-2X_p)]^3 = 0. \tag{41}$$

The EOS for β-equilibrium (npe) matter can be estimated by using the values of X_p, which can be obtained by solving Eq. (41). The properties of the neutron stars can be finally studied by solving Tolmann-Oppenheimer-Volkov (TOV) equations [33] with the derived nuclear EOS as an input.

III. Results and discussions

In order to make a comparison with the NL-RMF model [11, 12], the same saturation properties of nuclear matter and hadron masses are listed in Table I, which are used to determine the model parameters. The obtained model parameters are presented in Table II with the NL-RMF model parameters together for a comparison. The coupling constants are defined as $f_j = g_j^2/m_j^2$ ($j = \sigma$, ω, ρ, δ) in Refs. [11, 12]. The parameters of self-interacting terms in Table II are defined as $A = a/g_\sigma^3$ and $B = b/g_\sigma^4$.

Table I. Saturation properties of nuclear matter and hadron masses.

saturation properties	[12]
ρ_0 (fm^{-3})	0.16
E/A (MeV)	-16.0
K (MeV)	240.0
E_{sym} (MeV)	31.3
$M^\star/M$	0.75
M (MeV)	939
m_σ (MeV)	550
m_ω (MeV)	783
m_ρ (MeV)	770
m_δ (MeV)	980

Table II. Model Parameters in the VF-RMF and NL-RMF models.

Parameter	$VF-RMF$ model		$NL-RMF$ model [12]	
	$VF\rho$	$VF\rho\delta$	$NL\rho$	$NL\rho\delta$
g_σ	12.33	12.33	8.96	8.96
g_ω	10.52	10.52	9.24	9.24
g_ρ	4.01	6.80	3.80	6.93
g_δ	0.00	7.85	0.00	7.85
A (fm^{-1})	0.048	0.048	0.033	0.033
B	-0.021	-0.021	-0.0048	-0.0048

We use the obtained parameters in Table II to complete the calculations of self-consistence in the present work. The masses of hadrons (nucleons and mesons) in the medium can be obtained in the relativistic mean field approach (RMFA) with the VF effects by calculating the loop-diagrams in Fig. 1. We first come to the self-consistent calculations of in-medium meson masses. The obtained in-medium meson masses are presented in Fig. 2. It is obviously seen from Eqs. (16), (17) and (20), (21) that the in-medium mesom masses are related to the asymmetry parameter α. The results in Fig. 2 are for both cases of α=0.0 (symmetric matter) given by VFρ and α=1.0 (asymmetric matter) given by VF$\rho\delta$ models, respectively.

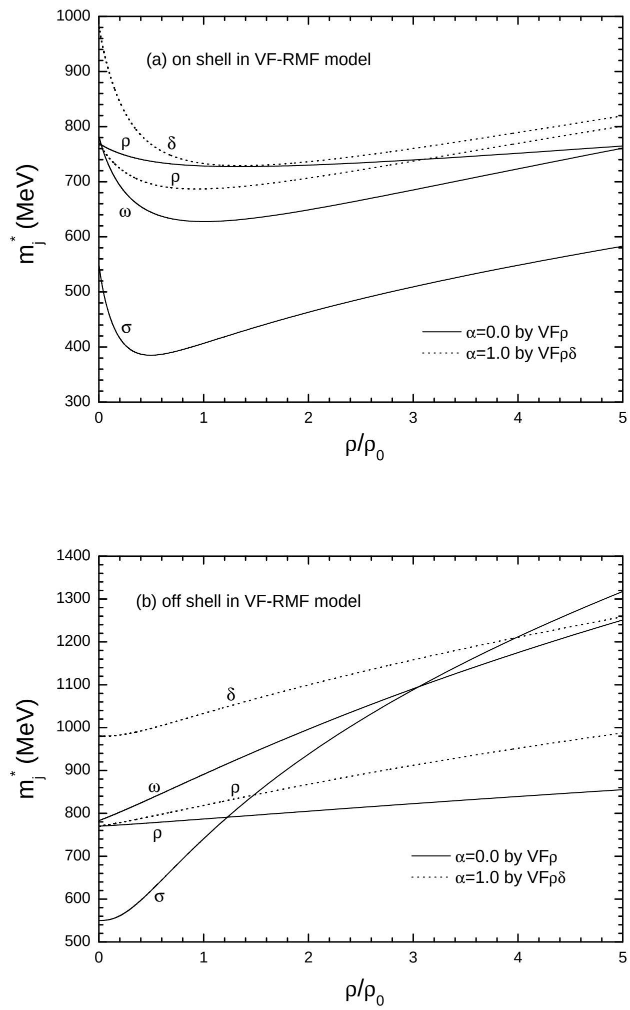

FIG. 2: Meson effective masses as a function of the baryon density in the VF-RMF model.

Fig. 2(a) shows the in-medium meson effective masses (on-shell: $\vec{q} = 0,\ q^0 = m_j^\star,\ j = \sigma,\ \omega,\ \rho,\ \delta$) as a function of the baryon density in the VF-RMF model. The in-medium modification to the masses of σ, ω, and ρ mesons have been studied in other theoretical models [20, 21, 22]. The in-medium effective mass decrease at the normal density is $\sim$18% for ρ and ω mesons in the model based on QCD sum rule [21]. The mass decrease is $\sim$20% for ω and ρ mesons at the normal density according to Brown-Rho (BR) scaling law [20]. In our model, the decreases of in-medium meson effective masses at the normal density are $\sim$25% for σ, $\sim$20% for ω, and only $\sim$5% for ρ mesons in the symmetric VFρ case, respectively. In the VF$\rho\delta$ case, the decreases of ρ and δ mesons are 11$\sim$13% and 25$\sim$27% at the normal density, respectively. Most experiments and theoretical approaches indicated a decrease of the in-medium meson effective masses around the normal density comparing with the masses at zero density [20, 21, 22, 23, 24, 25]. However, in the latest experiment [26], no significant mass shift for the ρ meson with momenta ranging from 0.8 to 3.0 GeV was observed. Up to now, the experimental results have not yet converged, and more work is needed to obtain consistent understanding of the in-medium behavior of vector mesons [34]. In general, the medium modifications to the masses of mesons are momentum dependent [35]. We note that the on-shell meson effective masses are obtained for the mesons at rest in our model. This is not in the momentum range of the CLAS experiment [26]. Until now, there is no experimental measurement about the in-medium modification to the mass of the δ meson. Our model indicates a significant decrease of the δ meson effective mass around the normal density. We note that the effective meson masses become to increase at high density regions in the

VF-RMF model. Unfortunately, the high density regions are beyond the reach of current experiments. It will be very interesting to test our prediction in the future experiments.

Fig. 2(b) shows the in-medium meson effective masses (off-shell: $q^\mu = 0$), which are used for the calculations of the nuclear EOS, as a function of the baryon density in the VF-RMF model. The off-shell meson masses are different from the on-shell meson masses because the four momenta carried by the meson propagators in these two situations are different. Since the meson propagators in the nucleon self-energy are computed at zero four momentum transfer (see Fig. 1(a)), we have to use the off-shell meson masses in the tadpole loop calculation for self-consistency.

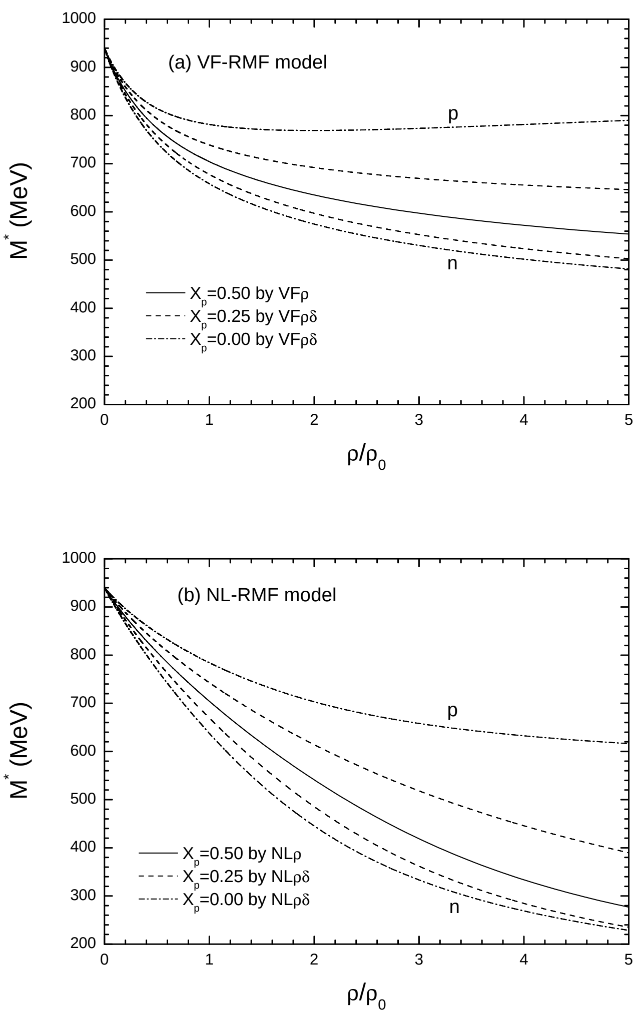

FIG. 3: Nucleon effective masses as a function of the baryon density in different models. The upper (lower) dashed and dash-dotted lines correspond to the masses of the proton (neutron). (a) VF-RMF model. (b) NL-RMF model.

The nucleon effective masses play an important role in the calculations of the EOS (see Eqs. (25) and (26)). We calculate the loop-diagram corrections to the self-energies of nucleons in medium. The nucleon effective masses without the δ meson can be calculated from Eq. (7). One can see from Eqs.

(12) and (13) that the presence of the δ meson leads to proton and neutron effective mass splitting. We present the baryon density dependence of proton and neutron effective masses for different proton fractions in the two models for a comparison in Fig. 3. The solid lines in Fig. 3 are the nucleon effective mass for symmetric matter (X_p=0.5).

Fig. 3(a) shows that the proton and neutron effective masses given by the VF$\rho\delta$ model decrease slowly with the increase of the baryon density, at variance with the NL$\rho\delta$ model that presents a much faster decrease (Fig. 3(b)). This main difference between the VF$\rho\delta$ and the NL$\rho\delta$ models actually comes from the in-medium meson masses (see Eqs. (22) and (23)). The in-medium meson masses (off-shell) increase with the increase of the baryon density in the VF-RMF model (see Fig. 2(b)). So it is natural that the VF effects lead to a slow decrease of the nucleon effective masses as the baryon density increases.

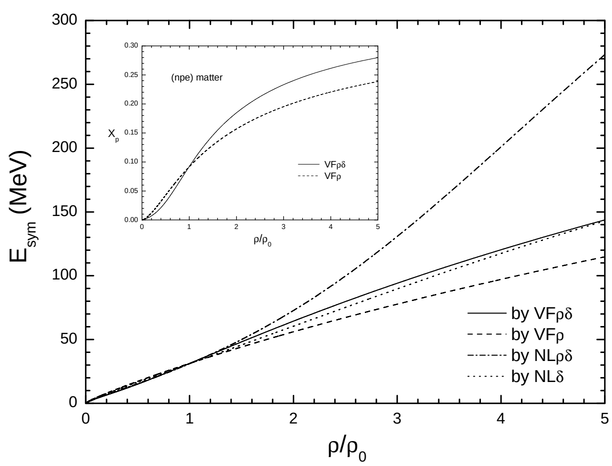

FIG. 4: The symmetry energy as a function of the baryon density in different models. The inset is the corresponding proton fraction.

The density dependence of the symmetry energy for the VF-RMF and NL-RMF models is presented in Fig. 4. We see a similar behavior of E_{sym} at saturation density for both the two models. With the increase of the baryon density, the symmetry energy given by the VF-RMF model increases slowly comparing with that given by the NL-RMF model. From Fig. 4 we see that the symmetry energy with the δ meson is stiffer than that without the δ meson for both the VF-RMF and the NL-RMF cases. The symmetry energy in the VF$\rho\delta$ case is softer than that in the NL$\rho\delta$ case. This is due to the VF effects. The presence of the δ meson affects the symmetry energy and consequently the EOS of asymmetric nuclear matter.

The β-equilibrium matter is relevant to the composition of the neutron stars. The EOS, pressure vs density, for (npe) matter in the VF-RMF and the NL-RMF models is presented together in Fig. 5 for a comparison. We see that the EOS in the VF-RMF is lower. Due to the VF effects, the EOS of asymmetric matter becomes softer.

In the present work, only two pictures for the neutron star composition are considered: pure neutron and β-equilibrium matter, $i.e.$ without strangeness bearing baryons and deconfined quarks (see Refs. [32, 36]). Furthermore, we limit the constituents to be neutrons, protons, and electrons in the latter

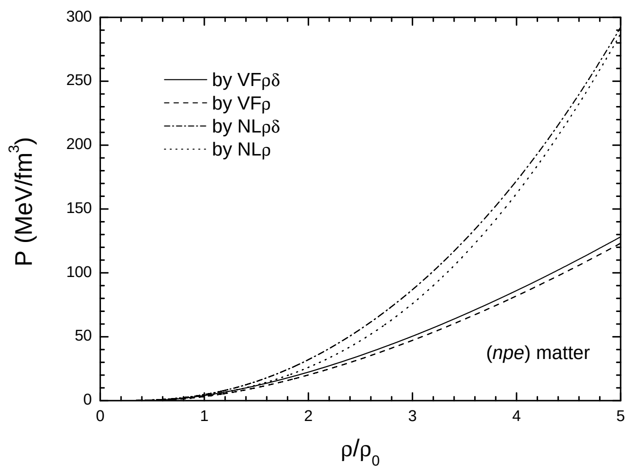

FIG. 5: Equation of state for (npe) matter.

case. In fact, in β-equilibrium matter, nucleons and electrons indeed dominate at low temperature.

The structure of neutron stars can be calculated by solving TOV equations. The correlation between the neutron star mass and the corresponding radius for the pure neutron and the β-equilibrium (npe) matter by the VF-RMF model are shown in Fig. 6. The obtained maxium mass, corresponding radius and central density are reported in Table III. We see from Fig. 6 and Table III that the VF-RMF model leads to the decrease of the neutron star masses for both the pure neutron and the (npe) matter. However, the NL-RMF model leads to heavier neutron stars (see Refs. [12, 16]). This is mainly because the EOS of asymmetric matter becomes softer since the symmetry energy becomes softer in the VF-RMF model.

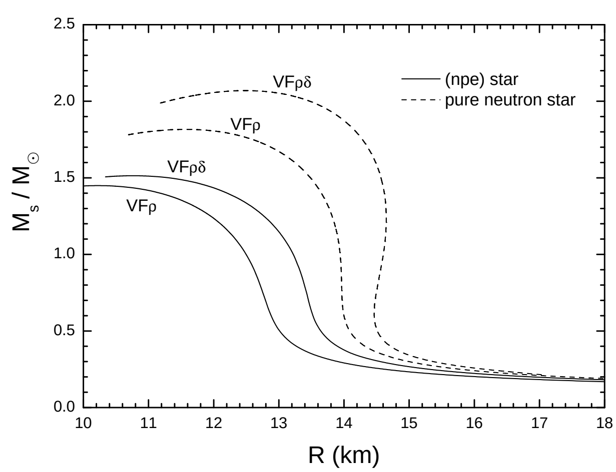

FIG. 6: The mass of the neutron star as a function of the radius of the neutron star.

We note that the coupling constant $f_j = g_j^2/m_j^2$ in the NL-RMF model is a constant fixed by the saturation properties of nuclear matter [11, 12]. In order to make a comparison, we define $F_j^\star = g_j^2/m_j^{\star 2}(\rho)$ (j=σ, ω, ρ, δ) in our model, here $m_j^\star$ is the off-shell meson mass. We are interested in the VF effects on the coupling constants. It is well known that the coupling constants in the DDRH model are density dependent (see [16]), whereas the meson masses are constant. In the present model, the coupling constants are constant, but the meson masses are density dependent. In order to distinguish, we define $F_j = g_j^{\star 2}(\rho)/m_j^2$ ($j = \sigma,\ \omega,\ \rho,\ g_j^\star$ is the coupling constant) for the DDRHρ case. We present a comparison between $F_j^\star$ and F_j in Fig. 7. We see from Fig. 7 that $F_j^\star$ decreases with the increase

Table III. The maximum mass, the corresponding radius and the central density of the neutron star in the VF-RMF model.

	$Model$	$VF-RMF$	
$neutron\ star$	$properties$	$VF\rho$	$VF\rho\delta$
$pure\ neutron$	$M_S/M_\odot$	1.82	2.07
	$R(km)$	11.57	12.49
	ρ_c/ρ_0	6.41	5.48
$(npe)\ matter$	$M_S/M_\odot$	1.45	1.51
	$R(km)$	10.22	10.77
	ρ_c/ρ_0	8.98	8.20

of the baryon density for both σ and ω mesons, which are due to the increase of the off-shell meson masses in high density regions. It shows that the variance trends of $F_j^\star$ and F_j are roughly the same for σ, ω, and ρ mesons. If we attribute the density dependence of the coupling constants in the DDRH model to the VF effects in our model, the density dependence of $F_j^\star$ and F_j should have the same physical origin.

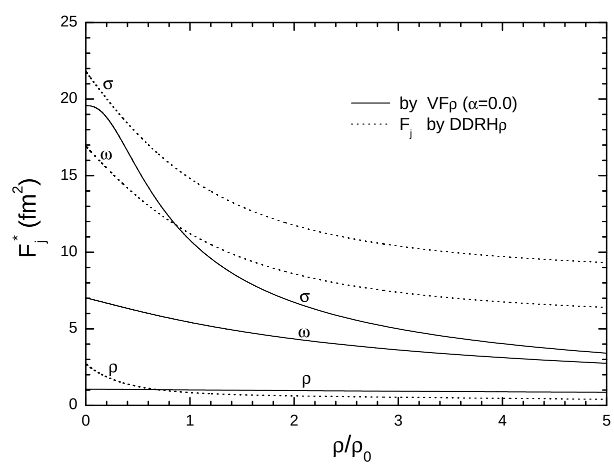

FIG. 7: A comparison between the ratio $F_j^\star$ and F_j.

IV. Summary

The VF corrections are investigated in the framework of the RMF approximation by using the relativistic Lagrangian density with the δ field in this work. By taking into account the loop corrections to the self-energies of the in-medium nucleons and mesons, the VF effects are naturally introduced into the RMF model. In order to make a comparison with the NL-RMF model, the same saturation properties of nuclear matter are used to determine the parameters of the VF model. We calculate the contributions from self-energy diagrams to the masses of the nucleons and mesons. The effective masses of the nucleons and mesons, especially the ρ and δ mesons, in the nuclear medium are obtained. We find that the nucleon effective masses decrease more slowly with the increase of the baryon density

comparing with the NL-RMF case. We also find that the dependence of the off-shell meson masses on the density in the medium is different from that of the on shell meson masses (see Fig. 2). The effects of the in-medium hadron masses on the nuclear EOS and the properties of the neutron stars are studied. The VF effects lead to softness of the symmetry energy and the EOS of asymmetric matter. Due to such softness, the neutron star masses are reduced quite a lot. This indicates that the VF effects on the neutron stars are important. We see from Fig. 2(b) that the off-shell in-medium meson masses increase with the increase of the baryon density. The off-shell in-medium meson masses can be used to calculate $F_j^\star$. The variance trends of $F_j^\star$ for σ, ω, and ρ mesons are roughly consistent with F_j in the DDRHρ case [16]. The density dependence behavior of the off-shell in-medium meson masses is very interesting indeed.

In the present work, we work in the Hartree approximation in which we only consider the dominant contributions from tadpole diagrams to the nucleon self-energy when we investigate the VF effects. In fact, the exchange diagram contributions can only provide small corrections to the EOS in the RMF approach at high densities [2]. It is well known that the symmetries of the infinite nuclear matter system can simplify the mean-field Lagrangian considerably. As pointed out in Ref. [2], when translational and rotational invariance of the nuclear matter is taken into account, the expectation values of all three-vector fields must vanish. Therefore, the expectation value of $\vec{G}_{\mu\nu}$ in Eq. (1) is zero and nonlinear ρ meson interactions (three or four ρ vertices) do not appear. Furthermore, since we only take into account the tadpole diagrams, only the neutral iso-vector meson (ρ^0) is involved in the nucleon self-energy diagrams even in the asymmetric nuclear matter ($\rho^\pm$ could contribute to the exchange diagrams which are ignored in the Hartree approximation).

It is suggested that the tensor coupling to the nucleon should be taken into account for the study of the vector mesons in nuclear medium [37]. In the present work, since we focus our attention on the VF effects on the properties of neutron stars, we do not include the tensor coupling effects in the calculations for the effective masses of the vector mesons. This will be studied in the future work, especially for the study of the ρ meson masses in the medium. Furthermore, the future study of the VF effects on the meson-nucleon coupling constants will be carried out. In addition, more careful study of the high density behavior of the meson-nucleon effective couplings, especially g_δ, is important and attractive.

Acknowledgments

This project is supported by the National Natural Science Foundation of China (Project Nos. 10675022 and 10875160), the Key Project of Chinese Ministry of Education (Project No. 106024), and the Special Grants from Beijing Normal University.

---

[1] J.D. Walecka, Ann. Phys. (N.Y.) **83**, 491 (1974).

[2] B.D. Serot, J.D. Walecka, Adv. Nucl. Phys. **16**, 1 (1986); Int. J. Mod. Phys. E **6**, 515 (1997).

[3] Y. Sugahara and H. Toki, Nucl. Phys. A **579**, 557 (1994).

[4] G.A. Lalazissis, J. König, and P. Ring, Phys. Rev. C **55**, 540 (1997).

[5] M.M. sharma, A.R. Farhan, and S. Mythili, Phys. Rev. C **61**, 054306 (2000).

[6] J. Boguta and A.R. Bodmer, Nucl. Phys. A **292**, 413 (1977).
[7] A.R. Bodmer, Nucl. Phys. A **526**, 703 (1991).
[8] H. Müeller and B.D. Serot, Phys. Rev. C **52**, 2072 (1995).
[9] R.J. Furnstahl and B.D. Serot, Nucl. Phys. A **671**, 447 (2000).
[10] H. Müeller and B.D. Serot, Nucl. Phys. A **606**, 508 (1996).
[11] B. Liu, V. Greco, V. Baran, M. Colonna, and M.D. Toro, Phys. Rev. C **65**, 045201 (2002).
[12] B. Liu, H. Guo, M.D. Toro, and V. Greco, Eur. Phys. J. A **25**, 293 (2005).
[13] D.P. Menezes and C. Providência, Phys. Rev. C **70**, 058801 (2004).
[14] T. Gaitanos, M.D. Toro, S. Typel, V. Baran, C. Fuchs, V. Greco, and H.H. Wolter, Nucl. Phys. A **732**, 24 (2004).
[15] V. Baran, M. Colonna, V. Greco, and M.D. Toro, Phys. Rep. **410**, 335 (2005).
[16] B. Liu, M.D. Toro, V. Greco, C.W. Shen, E.G. Zhao, and B.X. Sun, Phys. Rev. C **75**, 048801 (2007).
[17] C. Fuchs, H. Lenske, and H.H. Wolter, Phys. Rev. C **52**, 3043 (1995).
[18] F.D. Jong and H. Lenske, Phys. Rev. C **57**, 3099 (1998); F. Hofmann, C.M. Kell, and H. Lenske, ibid. **64**, 034314 (2001).
[19] S. Typel and H.H. Wolter, Nucl. Phys. A **656**, 331 (1999).
[20] G.E. Brown and M. Rho, Phys. Rev. Lett. **66**, 2720 (1991).
[21] T. Hatsuda and S.H. Lee, Phys. Rev. C **46**, R34 (1992).
[22] S. Sarkar *et al.*, Nucl. Phys. A **634**, 206 (1998).
[23] K. Ozawa *et al.*, Phys. Rev. Lett. **86**, 5019 (2001).
[24] D. Trnka *et al.* (CBELSA/TAPS), Phys. Rev. Lett. **94**, 192303 (2005).
[25] B. Krusche, Int. J. Mod. Phys. A **22**, 406 (2007).
[26] R. Nasseripour *et al.* (CLAS), Phys. Rev. Lett. **99**, 262302 (2007).
[27] A. Bhattacharyya, S.K. Ghosh, and S.C. Phatak, Phys. Rev. C **60**, 044903 (1999).
[28] H. Kurasawa and T. Suzuki, Nucl. Phys. A **490**, 571 (1988).
[29] W.D. Myers and W.J. Swiatecki, Ann. Phys. (N.Y.) **55**, 395 (1969).
[30] N.K. Glendenning, *Compact Stars, Nuclear Physics, Particle Physics and General Relativity* (Springer-Verlag, New York, Berlin, Heidelberg, 2000).
[31] H. Kouno, *et al.*, Phys. Rev. C **51**, 1754 (1995).
[32] J.M. Lattimer and M. Prakash, Science **304**, 536 (2004).
[33] R.C. Tolman, Phys. Rev. **55**, 364 (1939); J.R. Oppenheimer and G.M. Volkoff, Phys. Rev. **55**, 374 (1939).
[34] R.S. Hayano and T. Hatsuda, nucl-ex/08121702.
[35] M. Post, S. Leupold and U. Mosel, Nucl. Phys. A **741**, 81 (2004).
[36] C. Maieron, M. Baldo, G.F. Burgio, and H.J. Schulze, Phys. Rev. D **70**, 043010 (2004).
[37] R. Machleidt, K. Holinde and C. Elster, Phys. Rep. **149**, 1 (1987).